View Article Online
DOI: 10.1039/D0DT00356E

ARTICLE

Cu(I)-I coordination polymers as possible substitutes of lanthanides as downshifters for increasing the conversion efficiency of solar cells

Jésus López-Molina[a], Cecilio Hernández-Rodríguez[b], Ricardo Guerrero-Lemus[b], Eugenio Cantelar[c], Ginés Lifante[c], Marta Muñoz[d], and Pilar Amo-Ochoa*[a, e]

ABSTRACT: This work tries to contribute new solutions to increase the efficiency in the conversion of photons of the solar cells, by means of the use of photoluminescent Cu(I) coordination polymers (CPs), as possible alternative materials of lower cost, than those used in today, based on lanthanides. The selected CP of chemical formula $[Cu(NH_2MeIN)I]_n$ (NH_2MeIN= methyl, 2-amino isonicotinate), absorbs in the utraviolet and emits in the visible, being also easily nanoprocessable, by a simple and one pot botom-up approach. Nanofibers of this CP, can be embedded in organic matrices such as Ethyl Vinyl Acetate (EVA), forming transparent and homogenous films, with thermal stability up to approximately 150ºC. These new materials maintain the optical properties of the CP used as a dopant, ($[Cu(NH_2MeIN)I]_n$), with emission in yellow (570nm) at 300K, which is intensified when the working temperature is lowered. Additionally, these materials can be prepared with varying thicknesses; from a few microns to a few hundred nanometers, depending on the deposition method used (drop casting or spin coating respectively). The study of their external quantum efficiency (EQE) shows an increase in the UV range, which translates into an increase in conversion efficiency. Being the optimal CP concentration of 5% by weight in order to do not to diminish the transparency of the composite material. The calculated cost on the possible incorporation of this material to solar cells, show a 50% decrease over the cost reported in similar studies based on the use of lanthanides.

Introduction

A large scientific effort is being made from several years for increasing the conversion efficiency of solar cells by converting photons from the UV spectral range, where the external quantum efficiency (EQE) of solar cells is low.[1] This effort has been mostly based on the introduction of lanthanides[2] as downshifters directly into the bulk cell substrate[3] or on their as an added layer.[4] This second procedure is prevailing at present because of the low cost, easiness and potential to be integrated in the photovoltaic (PV) module lamination process.[5] Moreover, recent works show that the integration of such downshifters can increase the efficiency of standard Si-based solar cells up to 0.31%, without optimizing the optics of the device[6]. Also, this absorbing capacity of UV radiation prevents the undesirable degradation of some of the constituents of solar cells, thus improving the useful life of photovoltaic cells and increase the efficient potential of the solar cell. However, lanthanides are expensive, and a full range of alternative materials have been studied.[7] In this paper we propose a photoluminescent coordination polymer (CP) based on Cu(I) as possible sensitizer. From an economic point of view, copper is more abundant and less expensive than others metals and luminescent CPs based on Cu(I) are cheaper than others based on Ag(I) or Au(I). In addition, these soft metals show high polarizability to establish stable covalent bonds with soft ligands such as halides. In this context, CPs based on Cu(I)–I double chains have been shown to be a subfamily with remarkable optical properties but, even more importantly, with very sensitive and flexible structures[8]. Thus, the structures of these materials undergo slight structural changes under external physical and/or chemical stimuli, such as vapours, temperature and/or pressure, which significantly affecting their physical properties e.g. conductivity and/or emission.[9] [10] In particular, the photoluminescence of copper(I) halides with organic nitrogen-donor ligands has been extensively studied for performance as chemical [11] or biological sensors.[12] Although coordination polymers have not acquired great relevance at the industrial level, [13] the possibility of creating composite

[a] Facultad de Ciencias. Dpto. Química Inorgánica. Universidad Autónoma de Madrid 28049. Spain.
[b] Departamento de Física. Universidad de La Laguna. 38207 San Cristóbal de La Laguna. Spain.
[c] Facultad de Ciencias. Dpto. Física de Materiales, Universidad Autónoma de Madrid 28049. Spain.
[d] .Departamento de Matemática Aplicada, Ciencia e Ingeniería de los Materiales y Tecnología Electrónica. Universidad Rey Juan Carlos. Madrid 28933, Spain
[e,f] Institute for Advanced Research in Chemical Sciences (IAdChem). Universidad Autónoma de Madrid. Madrid 28049, Spain

Electronic Supplementary Information (ESI) available: Tables of Crystallographic data, X-ray powder diffractograms, emission spectra and additional Figures. See DOI: xxxx

materials using coordination polymers with an organic matrix, as for example Ethyl Vinyl Acetate (EVA), can give rise to a new range of materials that retain the intrinsic optical properties of coordination networks.[9] The CP studied in this work [CuI(NH_2-MeIN)]$_n$ (NH_2-MeIN= methyl, 2-amino isonicotinate) has an absorption band in the ultraviolet region and although it shows low emission at 25 ˚C, the intensity of the emission increases by lowering the temperature. In addition, this one-dimensional coordination polymer can be instantaneously nanoprocessed by bottom-up approximation, in a simple direct synthesis at room temperature, which will allow to create composite materials of nanometric thicknesses with similar functionality and much lower cost. Therefore, the incorporation of Cu(I) coordination polymers of nanometric size in solar cells allows a new demand for innovative and intelligent materials to be introduced into the market as an alternative option to the rare earth monopoly.

Results and discussion

Synthesis of composite materials [Cu(NH_2-MeIN)I]$_n$@EVA.

The coordination polymer 1D-[Cu(NH_2-MeIN)I]$_n$ (Fig. 1), has been successfully obtained in nanometric dimensions[9] by instantly direct synthesis between CuI and methyl-2-aminoisonicotinate (NH_2-MeIN) in a mixture acetonitrile:ethanol at room temperature (Sec. S1, Fig. S1). This coordination polymer presents interesting optical properties that make it an excellent candidate for the study carried out in this work: (i)The CP shows emission in yellow at 300K, which intensifies strongly when the temperature decreases (80 K)[9] as a result of an increase in its structural rigidity and therefore a constraint or decrease in its bond distances.[14]

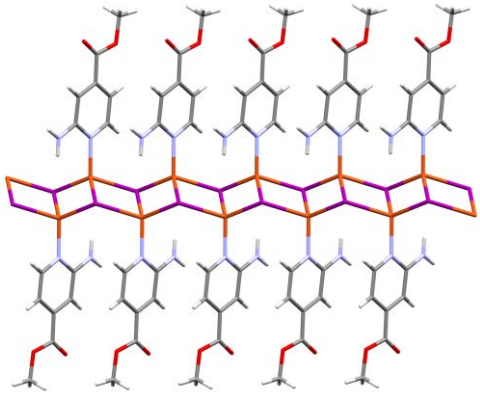

Figure 1. Fragment of the crystal structure of CP **1D-[Cu(NH_2-MeIN)I]$_n$** solved by single crystal X-ray diffraction at 296K[9]. Orange: Cu, purple: I, blue: N, black: C, red: O, grey: H.

In addition, the CP absorbs around 350 nm (ultraviolet) (Fig. S8). These characteristics make it an interesting compound to manufacture the new composite materials.

As solar panels must work outdoors in ambient conditions, their components must have a series of characteristics that allow it to withstand the weather. EVA has been chosen in the study due to its capacity of withstanding very extreme temperatures. In addition, it is highly transparent to allow solar energy to reach the photovoltaic cell without significant absorption and also has flexibility and high impact resistance to protect the cells from possible mechanical damages. Moreover, it is able to provide electrical insulation to avoid the risk of fire and has thermal stability, being the standard encapsulatio
photovoltaic industry.[15] All of these characteristics will extend the life of the panel, beyond 25 years, and protect it from external agents such as moisture or dust.

The manufacture of the composited materials at different proportions of the nano coordination polymer (5-30% wt) was done dissolving the EVA in trichloroethylene (TCE) at 85 °C and over this solution, different amounts (by weight) of [Cu(NH_2-MeIN)I]$_n$ were added. Both components were mixed and dispersed by sonication tip (Fig. 2a). The X-ray powder diffraction and IR spectra of composite materials with different proportions of the CP (5-30% wt) shows that the synthesis conditions used for the creation of these materials do not alter the structure of the CP within the organic matrix (EVA) (Fig. S4-S5).

Figure 2: (a) Schematic synthesis to prepare thin films of **[Cu(NH_2-MeIN)I]$_n$@EVA (5-30% wt)** and deposition over SiO_2 surfaces by drop casting. (b) Schematic procedure of

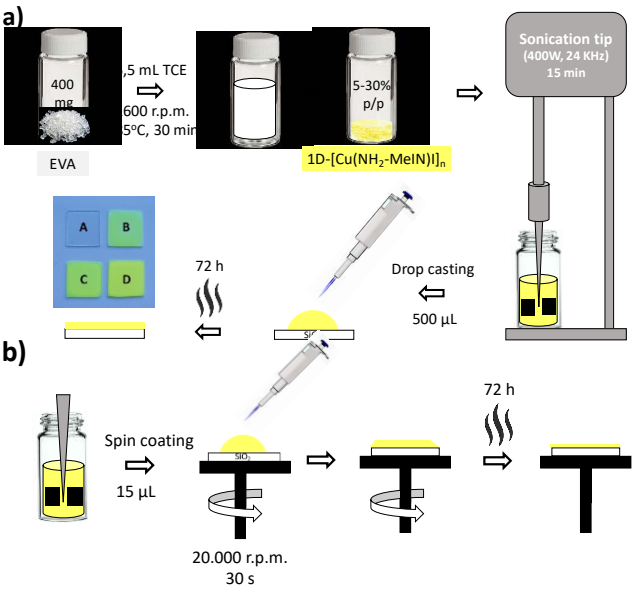

[Cu(NH_2-MeIN)I]$_n$@EVA (5-30% wt) composites deposited on SiO_2 surfaces by spin-coating.

The homogeneity of the composite materials [Cu(NH_2-MeIN)I]$_n$@EVA was also studied by SEM-EDX. In the material prepared only with EVA (Fig. S9A), a high C and O content is identified, corresponding to the elemental composition of EVA organic polymer. After incorporating 5, 10 and 15 % (wt.) of coordination polymer [Cu(NH_2-MeIN)I]$_n$ (Fig. S9B-D), the spectrum identified a constant ratio 1:1 (Cu:I) content in each hybrid material manufactured. In addition, TXRF made over the **[Cu(NH_2-MeIN)I]$_n$@EVA-5%** corroborates a homogeneous distribution of CP (Fig. S10).

The thickness of composite materials is regulated by two different deposition methods. In the case of requesting micrometric thickness films, the deposition of these suspensions on SiO_2 was carried out by drop casting, obtaining films of around 2.0x2.0x0.2 mm dimensions (Fig. S23A-E). If the thickness of the films is required to reach nanometer or sub-micrometer scale, spin coating is used, obtaining films of around 150 nm thickness (Fig. 3).

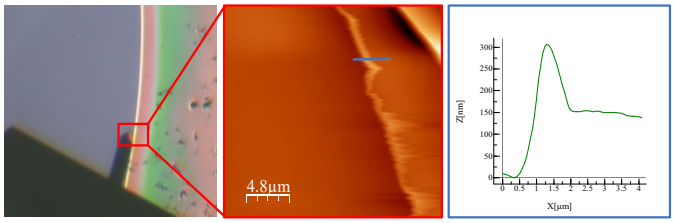

Figure 3: AFM images showing sub-micrometer thickness of the **[Cu(NH$_2$-MeIN)I]$_n$@EVA-5% wt** composite film, deposited on SiO_2 surfaces by spin-coating.

Composite materials [Cu(NH$_2$-MeIN)I]$_n$@EVA, thermal stability.

As shown in the Fig. 4 and Fig. S6, the thermogravimetric analysis of EVA, 1D-[Cu(NH$_2$-MeIN)I]$_n$ and [Cu(NH$_2$-MeIN)I]$_n$@EVA, respectively have been carried out, in order to know the thermal stability of the CP after embedding it in the EVA organic matrix. The EVA thermogram shows two stages of thermal decomposition. The first mass loss of 19%, observed from 300 to 400 °C, corresponds to the deacetylation of the vinyl group, which results in the production of acetic acid in the gaseous state and the formation of carbon-carbon double bonds throughout of the polymer chain. The remaining mass loss, observed from 400 to 500 °C, corresponds to the thermo-oxidation of the unsaturated chains and to the volatilization by rupture of the double bonds.[16] The thermogram of 1D-[Cu(NH$_2$-MeIN)I]$_n$, shows a first thermal decomposition from 150 to 250 °C with a mass loss of 44%, corresponding to the decomposition of methyl-2-aminoisonicotinate (NH$_2$-MeIN). The second loss takes place from 400 to 700 °C, corresponding to remains of volatile copper-iodine compounds. The thermogravimetric analysis of [Cu(NH$_2$-MeIN)I]$_n$@EVA-5-15% (Figs 4, S6c-e and S7) shows that the incorporation of the coordination polymer in EVA does not affect the thermal stability of the reinforcement matrix.

Further, the first thermal decomposition of the composite material, around 150 °C, is close to the maximum thermal stability limit necessary for the integration process in photovoltaic (PV) minimodules.[17] Then, this study shows that [Cu(NH$_2$-MeIN)I]$_n$@EVA thin films could be incorporated in any step of the minimodule assembly, since this process is usually carried out at temperatures close to 150 °C.

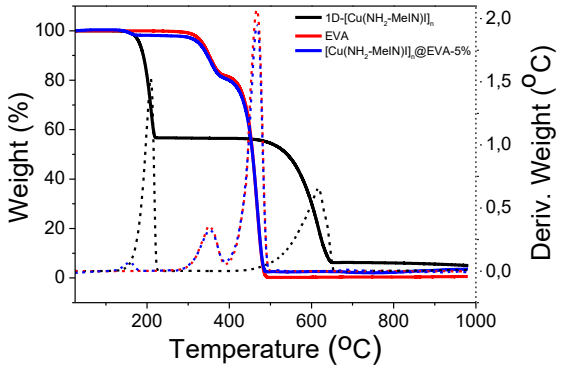

Figure 4. Thermogravimetric analysis coupled to differential thermal analysis (TGA-DTA) of **1D-[Cu(NH$_2$-MeIN)I]$_n$** (black line), **EVA** (red line) and **[Cu(NH$_2$-MeIN)I]$_n$@EVA-5%** thin film (blue line) in a temperature range from 25 to 1000 °C, under nitrogen gas with flow rate of 90 mL/min and heating rate of 10 °C/min, in a range temperature from 25 to 1000 °C.

Composite materials [Cu(NH$_2$-MeIN)I]$_n$@EVA, luminescence properties.

The compound 1D-[Cu(NH$_2$-MeIN)I]$_n$, selected to be introduced into the organic matrix (EVA) has temperature-dependent luminescent behaviour.[9] At 300 K, and after excitation with λ_{exc}= 365 nm, [Cu(NH$_2$-MeIN)I]$_n$ has a weak yellow emission with an asymmetric band centred at λ_{em}= 550 nm, while upon cooling the temperature from 300 to 80 K, exhibits a progressive increase in its emission intensity without shifting of the main band. This process is reversible and thus warming up the materials from 80 K to 300 K produces a gradual recovery of their initial properties, which makes it a temperature-dependent luminescent material.[9] This increase in emission intensity as the temperature decreases can be explained based on the crystalline structure solved at 296 and 110 K by single crystal X-ray diffraction (Table S1). Although the unit cell coincides with both temperatures, the flexibility of the double chains Cu(I)-I makes the coordination polymer behave like a true 'molecular spring', given that the distances Cu-I and Cu···Cu (Å) are shortened and the angles I···Cu···I (°) are contracted when the temperature decreases (Table S2), due to an increase in the structural rigidity of the compound. The emission centered around (550-570 nm) can be most likely due to a mixed iodine to ligand and metal to ligand charge transfer (IL/ML(CT) [3(I + M)LCT].[18]

When 1D-[Cu(NH$_2$-MeIN)I]$_n$ is embedding in EVA, a naked eye experiment of [Cu(NH$_2$-MeIN)I]$_n$@EVA under UV lamp (λ_{exc}=312 nm) at 80 K showed that [Cu(NH$_2$-MeIN)I]$_n$@EVA-15% film deposited in SiO_2 emits in the yellow region very intensely, showing that the new composites materials retaining the luminescent properties of the coordination polymer, thus creating a photoluminescent composite with temperature response (Fig. 5 and Figs. S18-20).

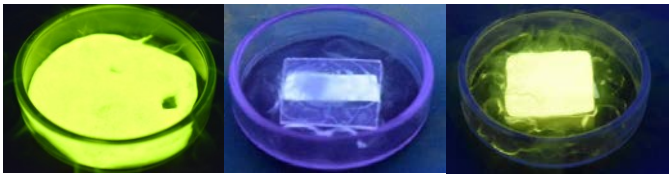

Figure 5. Emission in a naked eye experiment under UV lamp (λ_{exc}=312 nm) at 80 K of **1D-[Cu(NH$_2$-MeIN)I]$_n$** (left), **EVA** (middle) and **[Cu(NH$_2$-MeIN)I]$_n$@EVA-15%** (right) composite film deposited on SiO_2 surfaces.

The emission spectra of the new composite materials ([Cu(NH$_2$-MeIN)I]$_n$@EVA-5-30%) (λ_{exc}= 400 nm), have a very weak band (low intensity) at room temperature, which increases as the temperature drops, reaching a maximum around 570 nm at 80K (Fig. 6). This behavior is analogous in all composite materials regardless of the concentration of the added CP (5, 10, 15, 30%), (Fig. S11-20). This process is reversible and thus warming up the materials from 80 K to 300 K produces a gradual recovery of their initial properties. These results show, as we have already mention, that the new composite materials retain the optical properties of the selected CP.

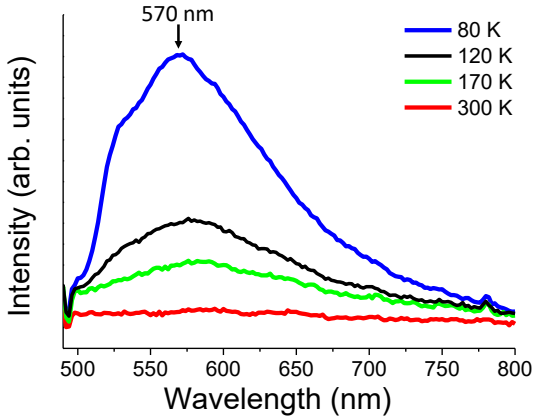

Figure 6: Emission spectrum of **[Cu(NH$_2$-MeIN)I]$_n$@EVA-5%** after excitation at 400 nm, at different temperature, from 298K (red line) to 80K (blue line).

Composite materials [Cu(NH$_2$-MeIN)I]$_n$@EVA: Transparency and Mechanical Properties.

One of the advantages of preparing composite materials is that their manufacturing involves an improvement in the mechanical properties of the coordination polymer. As shown in Figs. 7 and S21, the micrometric thickness film prepared only with the EVA organic matrix allows to obtain a flexible and transparent material. The degree of processability is maintained even after embedding 30% of [Cu(NH$_2$-MeIN)I]$_n$ in the organic matrix (Fig. 7 (4-6)), retaining in any of the cases almost the original flexibility of EVA. However, the transparency degree in the film Cu(I)-EVA decreases dramatically when the content of the coordination polymer in the organic matrix was increased.

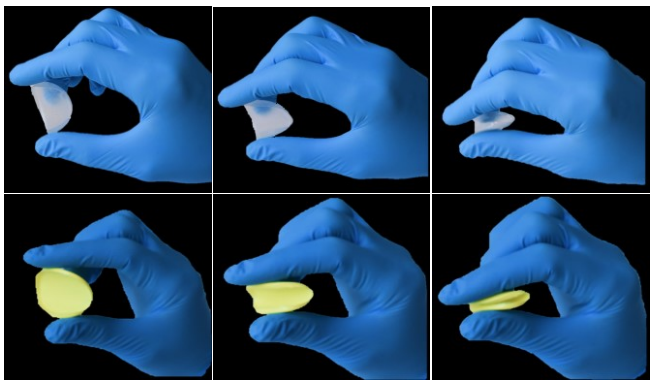

Figure 7. Flexibility degree in a naked eye experiment under visible light at 296K of **EVA** (first row: images 1-3) and **[Cu(NH$_2$-MeIN)I]$_n$@EVA-30%** thin films (second row: images 4-6).

The UV/Visible absorption study (Fig. S22) shows that the opacity of the prepared composite materials increases with the increase in the concentration of the coordination polymer on EVA. The film made only with EVA, used as a reference target, almost does not absorb radiation in the range of 190-1100 nm, due to its high transparency. When 5% of 1D-[Cu(NH$_2$-MeIN)I]$_n$ is incorporated onto EVA, the composite absorbs almost all the incident radiation. A higher weight percentage of coordination polymer selected (10, 15 and 20% wt), shows that the absorbance signal in the composite materials is saturated because the opacity of the film is becoming more marked. In principle, these results presuppose an inconvenient for External Quantum Efficiency (EQE) measures, since the transparency of the films is an indispensable requirement for the measures to be legible.

The tensile test curves of the [Cu(NH$_2$-MeIN)I]$_n$@EVA composites are plotted in Fig. 7. The tensile test was also performed on the pristine EVA polymer for comparison. From the Stress-Strain curves we can see the influence of different concentration of [Cu(NH$_2$-MeIN)I]$_n$ reinforcement on the EVA mechanical properties.

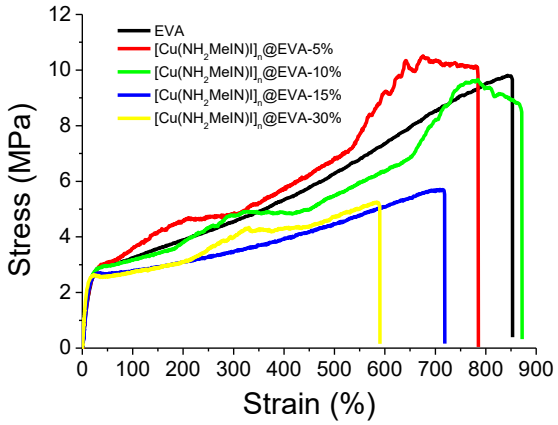

Figure 8. Stress-Strain curves of pristine EVA and [Cu(NH$_2$-MeIN)I]$_n$@EVA composites.

The load increases linearly with a high slope at first, and then it increases more gradually. Mechanical properties are listed in Table S4. Films fabricated with the highest concentration of nanofibers show a very slightly higher rigidity directly connected with this increment in the Elastic Modulus value.

The results revealed that the incorporation of $[Cu(NH_2\text{-MeIN})I]_n$ decreases the fracture strength value (σ_u) proportionally to the $[Cu(NH_2\text{-MeIN})I]_n$ content, achieving the lowest values of fracture strength of nearly 5.72 and 5.51 MPa at 15% and 30%, respectively (Table S4). That seems to be related to a weak interaction at the matrix-reinforcement interface in the composite. At high concentrations, 10%, 15% and 30% (wt.), probably nanofibers can form agglomerates decreasing their interactions with the polymeric matrix. On the other hand, fracture strain values decrease with the increment of the concentration of the reinforcement, achieving a minimum value, 603%, at the highest concentration 30% (wt.) with a wide range of variability, mainly due to the poor adhesion between the nano-reinforce and the EVA matrix. The addition of different amounts of nanofibers to the EVA matrix does not alter the Elastic Modulus value of the nanocomposite. This can be also due to the weak interaction between EVA matrix and $[Cu(NH_2\text{-MeIN})I]_n$ reinforcement. Essentially, the tensile test shows that up to 5% by weight compositions of the CP in the EVA, it does not suffer drastic changes in its fracture strength and fracture strain, nor in the Elastic modulus. So this composition which is the ideal, in terms of transparency and EQE (see below), would also maintain the mechanical properties of the matrix.

Composite materials $[Cu(NH_2\text{-MeIN})I]_n$@EVA: External Quantum Efficiency (EQE) measurement.

The influence of the composite material on the solar reference PV cell is evaluated by EQE, that is, by the fraction of incident photons that reach the solar cell and produces an electron-hole pair in the external circuit under short-circuit conditions.[19] The EQE spectra, exposed in Fig. 9, show values for a PV minimodule covered by glass and EVA and compared, under the same conditions, with the same minimodule placing the different luminescent film embedded in EVA at different concentrations. When the $[Cu(NH_2\text{-MeIN})I]_n$@EVA-5% film is incorporated on the Si photovoltaic minimodule, a slight increase in the UV spectral range (300-380 nm) is observed with respect to the PV mini-module covered only with the bare glass, whose EQE value is close to zero. The lowering of EQE in the Visible region by incorporating the film on the photovoltaic minimodule (substantial in the short wavelengths region of the visible range) is due to the increase in opacity of the EVA+Cu-based film when the film concentration is increased. Of all the luminescent films deposited, $[Cu(NH_2\text{-MeIN})I]_n$@ EVA-5% is the only one that shows an appreciable increase in the value of EQE in the UV region also because below this percentage the conversion process is negligible, and above this percentage the increase in opacity also affects the UV spectral range avoiding the transmittance of the shifted photons to the solar cell. Also, it is important to mention that the integration of the downshifter has not been optically optimized by encapsulating it to the minimodule. This is due to the need to use the same minimodule for appropriately comparing the EQE spectra with the different samples. Nevertheless, since an increase in the value of EQE in the UV region translates into an increase in conversion efficiency, it becomes clear that $[Cu(NH_2\text{-MeIN})I]_n$ is an active species with an interesting potential for its application in solar cells, since it is capable of moving the photons of the incident radiation (UV region) to longer wavelengths where the Si solar cell shows higher conversion efficiency (Visible region), avoiding absorption and reflection losses of the photons , as well as parasitic absorptions[19], [20] [21] and also preventing the undesirable degradation of EVA, thus improving the useful life of photovoltaic cells and increase the efficiency of the solar cell.[22],[23] Thus, the values of EQE are expected to increase in the UV range as the concentration of $[Cu(NH_2\text{-MeIN})I]_n$ increases in the organic matrix to the limit of solubility or luminescence saturation, as it has been described elsewhere.[17, 20] It is necessary to emphasize that the thickness of the luminescent film affects the EQE result, since it is linked to an increase in absorption in the UV range and, to a lesser extent, a lower transmittance of the film. This affection can be considered very similar to variations in the active species concentration in the film. In future works we will define a protocol to optimize thickness and active species concentration in the film, also taking into account that the deposition procedure must remain simple to be competitive for being adapted to the PV industry.

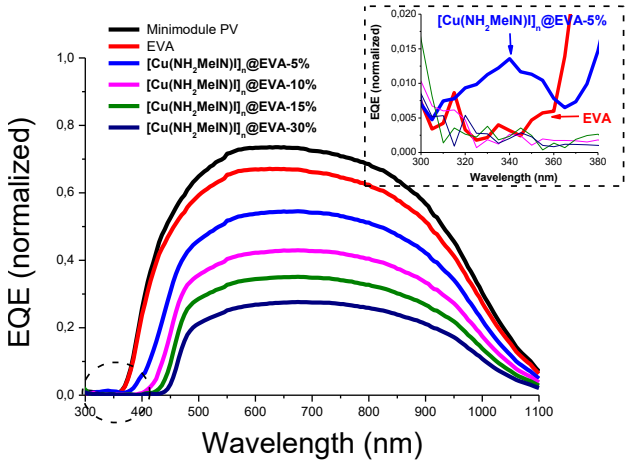

Figure 9. External Quantum Efficiency (EQE) spectrum collected for **EVA** (red line), **$[Cu(NH_2\text{-MeIN})I]_n$@EVA-5%** (light blue line), **$[Cu(NH_2\text{-MeIN})I]_n$@EVA-10%** (pink line), **$[Cu(NH_2\text{-MeIN})I]_n$@EVA-15%** (green line) and **$[Cu(NH_2\text{-MeIN})I]_n$@EVA-30%** (dark blue) thin-films deposited in Si photovoltaic mini module, in a wavelength range from 300 to 1100 nm at room temperature. Inset figure: Extension of the wavelength zone between 300 and 380 nm.

Composite materials $[Cu(NH_2\text{-MeIN})I]_n$@EVA: Industrial cost estimation.

Based on the increase in energy efficiency registered in the photovoltaic cell after incorporating the luminescent films, as well as the high processability and the low environmental impact of manufacturing these novel copper(I)-based composite materials, has been calculated the additional cost that involves the incorporation of these films in the integration of new solar cells.

To date, luminescent active species based on rare earths have been taken into account as Eu^{3+} ([19, 24] [6]) or Gd^{3+} [6], or dyes.[25] In this work, the incorporation of a transition metal d^{10} as a metallic center, copper in this case, makes possible to reduce the costs considerably if the expected increase in EQE in the UV range is appreciable and the decrease of EQE at larger wavelengths due to increases in opacity is avoided. The current price in the copper iodide wholesale market is around 8€/kg,

and the cost of the organic ligand is 0.90€/Kg. Taking into account the stoichiometry, the synthesis yield and the solvent expense, the price involved in the synthesis of the coordination polymer $[Cu(NH_2\text{-MeIN})I]_n$, is 9.09€/kg. Knowing that the cost of the organic matrix (EVA) is 1.5 € / Kg and that to make a composite film EVA and of $[Cu(NH_2\text{-MeIN})I]_n$ at 5% by weight, 20.0 mg of coordination polymer is needed, the global expense to manufacture a sheet of micrometric thickness is 0.041 €/m^2, a half of the expected costs reported with lanthanides in the literature.[26]

Conclusions.

Based on the requirements necessary to obtain a response in the photovoltaic cell, coordination polymers (CPs) based on CuI with pyridine derivatives can be an interesting new family of compounds, that thanks to their optical properties and their low cost, compared with the rare earth, should be used as substitutes of lanthanides as downshifters for increasing the conversion efficiency of solar cells.

In this work, 1D-$[Cu(NH_2\text{-MeIN})I]_n$ has been selected as an active specie, since absorbs in the ultraviolet region and present yellow emission. In addition, its nanoprocessing is very simple thanks to its high insolubility in the reaction medium. For these reasons, it has been selected for the creation of new micro or ultrathin (nano) composite materials films with EVA as an organic matrix. The new composite materials maintain the optical properties of the CP and at low concentrations of CP (5%) also maintain a high degree of transparency, the EVA mechanical properties, even the thermal decomposition, is close to the maximum thermal stability limit necessary for the integration process in photovoltaic minimodules. In addition, $[Cu(NH_2\text{-MeIN})I]_n$@ EVA-5% shows an appreciable increase in the value of EQE in the UV region.

This study, opens the door to the possibility of design new cheaper composite materials based on this wide family of CuI double-chain CPs, selecting those that present in addition to UV absorption, high emission intensity in the Visible region at 300 K. The degree of transparency can be modified playing with the thickness and the amount of CP on the composite materials, among other factors.

Experimental

Materials and methods

All reagents and solvents purchased were used without further purification. The reagents used in the synthesis, copper Iodide (I) and methyl-2-aminoisonicotinate, were purchased from Sigma Aldrich (CAS: 7681-65-4 and 14667-47-1). The solvents used in the synthesis, acetonitrile and ethanol, are purchased in VWR with HPLC purification grade. Poly-(Ethylene Vinyl Acetate) (EVA) was purchased at Sigma-Aldrich, with 25% vinyl acetate and 400-900 ppm of BHT as an inhibitor. Trichlorethylene (TCE) was purchased in Panreac and is stabilized in EtOH. TCE was used to improve the dissolution of hot EVA.

The dispersion of the coordination polymer in EVA organic matrix was carried out with a sonication tip Hielscher UP400S (power: 400W, frequency: 24 KHz). IR spectra were recorded with a PerkinElmer 100 spectrophotometer using a universal attenuated total reflection (ATR) sampling accessory from 4000 to 650 cm^{-1}. Elemental analyses were performed with a LECO CHNS-932 Elemental Analyzer. Powder X-ray diffraction data was collected using a Diffractometer PANalytical X'Pert PRO with θ/2θ primary monochromator and X'Celerator fast detector and monochromator 1° for $K_{\alpha 1}$. The samples have been analyzed with scanning θ/2θ, from 3-60 degrees, with an angular increase of 0.0167 and a time per increment of 100 s. Thermogravimetric analyses (TGA) were carried out on a TA Instruments Q500 thermobalance oven with a Pt sample holder. Experiments were carried out under nitrogen gas with flow rate of 90 mL/min and heating rate of 10 °C/min, in a range temperature from 25 to 1000 °C. The transparency of hybrid materials was measured by UV-visible absorption, using an Agilent 8452 diode array spectrophotometer over the solid samples at room temperature. The spectra were collected in a wavelength range from 190 to 1100 nm. Scanning Electron Microscopy (SEM) images were taken in a JMS 6335F electron microscope, applying an electron beam of 300 μA intensity and 15.0 kV potential, at a pressure of 10^{-7} Pa. After sample preparation, the films were metallized with a 15 nm thick Au layer, at a pressure of 10^{-3} Pa. SEM-EDX images and EDX spectra were taken in a Hitachi S-3000N microscope with an ESED coupled to an INCAx-sight EDX analyser. For this technique, the samples were metallized with a gold layer of 15 nm, under a pressure of 10^{-3} Pa. Atomic Force Microscopy images were registered in a Nanotec Electronica microscope, at room temperature and in an open atmosphere, using Olympus cantilevers with a constant nominal force of 0.75 N/m. Images were processed by the use of the WSxM program. The analysis by TXRF was performed using a TXRF 8030C spectrometer (Cameca, France), equipped with a 3 kW X-ray tube with a Mo/W alloy anode with a double-W/C multilayer monochromator, adjusted to obtain an excitation energy of 17.4 keV (Mo-K_α), for Cu and I evaluation, and a Si(Li) detector with an active area of 80 mm^2 with a resolution of 150 eV at 5.9 KeV (Oxford Instruments, England). The measurements were performed working at 50 kV, and the intensity was adjusted automatically so that a count rate of about 8500 cps was achieved. A fixed acquisition time of 500 s was used. The photovoltaic (PV) device where the downshifter is placed is a PV mini module based on a single p-type mc-Si solar cell (non-textured and with a SiNx antireflection coating optimized at 600 nm) encapsulated in a standard solar glass and showing a 16% conversion efficiency. A standard EQE setup based on a 100W Xe arc lamp, a monochromator and a digital lock-in amplifier has been used. The PV mini-module is fixed in the EQE setup to assure the reproducibility of results between samples. Also, the glass substrates with EVA and with or without the downshifter are fixed on top of the mini-module.

Excitation and emission spectra. The excitation spectra were performed by using a 450 W Xe lamp attached to a Digikröm CM-110 monochromator with 110 mm focal length. The thermal dependence of the luminescence emission spectra of

films were performed with an ARC Spectrapro 500-I monochromator with 500 mm focal length, and then detected with a photo-multiplier tube, where a long pass filter was placed at the entrance slit of the monochromator to block the excitation light. Measurements at variable temperature were done with an Oxford Cryostat Optistat DN.

Synthetic procedures

Synthesis of 1D-[Cu(NH_2-MeIN)I]$_n$. The synthesis procedure of the coordination polymer (CP), as well as its structural description, has been reported previously.[9] CP was obtained by stoichiometric reaction between CuI (100 mg, 0.53 mmol) and methyl-2-aminoisonicotinate (81 mg, 0.53 mmol) at 25 ° C and under magnetic stirring (500 r.p.m.), using a mixture acetonitrile: ethanol (1: 1) in the minimum amount possible to facilitate instantaneous precipitation of the reaction product. A pale-yellow solid is immediately formed, filtered off, washed with acetonitrile (2 x 5 mL), ethanol (2 x 5 mL) and diethyl ether (2 x 3 mL), and dried in vacuum. Single crystals were formed upon standing the mother yellow solution at 25 ºC for 72 h (Yield: 85 mg; 50 % based on Cu). Elemental analysis calcd (%) for $C_7H_8CuIO_2N_2$: C 24.52, H 2.34, N 8.17; found: C 24.96, H 2.34, N 8.07; IR selected data (ATR): n (cm-1) = 3450 (s), 3345 (s), 3186 (w), 3078 (w), 2992 (w), 2945 (w), 2845 (w), 1788 (w), 1716 (vs), 1634 (vs), 1603 (m), 1560 (vs), 1489 (w), 1448 (vs), 1432 (s), 1346 (m), 1308 (vs), 1270 (vs), 1249 (s), 1123 (s), 999 (s), 900 (m), 830 (w), 816 (m), 762 (vs), 737 (m), 697 (w). The powder X-ray diffraction (PXRD) data to compound confirmed the purity of both crystals and solid.

Preparation of composite thin film [Cu(NH_2-MeIN)I]$_n$@EVA. Ethyl vinyl acetate (EVA) polymer was doped with coordination polymer 1D-[Cu(NH_2-MeIN)I]$_n$ in 5, 10, 15 and 30% (wt). 0.400g EVA was dissolved in 5.5 mL of trichlorethylene (TCE) at 85 °C for 30 minutes, under magnetic stirring (1600 rpm). Over this solution 20.0, 40.0, 60.0, 80.0 and 120.0 mg of [Cu(NH_2-MeIN)I]$_n$ were added, respectively. Both components were mixed and dispersed by sonication tip for 15 minutes at 25 °C (65% amplitude). By drop-casting, 500 µL of the resulting homogeneous dispersion was deposited on SiO_2 surfaces (20 × 20 × 2 mm) and dried in air for 48 h to remove TCE by low evaporation. This solution amount is enough to obtain a micrometric thickness films that completely covers the glass, which are optimum for the EQE experiments. Finally, the glass is directly placed on a PV mini module, and illuminated for measuring the External Quantum Efficiency (EQE). The rest of the suspension is deposited in a Petri dish to obtain a film that allows the structural characterization of the composite thin film. IR, PXRD, TGA, SEM-EDX and emission spectral data showed the presence of [Cu(NH_2-MeIN)I]$_n$ in the films.

Preparation of composite sub-micrometer thin film [Cu(NH_2-MeIN)I]$_n$@EVA.
15 µL of the dispersed material was supported on SiO_2 surfaces by spin-coating for 30 seconds at 20000 rpm and dried with an Argon flow for 3 minutes, obtaining a sheet of nanometric thickness which was confirmed by AFM (Fig. 3).

Mechanical characterization of film [Cu(NH_2-MeIN)I]$_n$@EVA.
Tensile tests were performed on a MTS Alliance RT/5 testing machine (URJC, LATEP) equipped with a 500 N load cell at 23ºC and 50% humidity, according to the method 35 PP (ISO 527)_5A SIN. For each condition, at least three samples of each concentration were tested at a strain rate of 10 mm/min. The films were cut with a CEAST die cutting machine in dumbbell shape 13x1.9 mm (Fig. S24) and the thickness, controlled by the processing step, is close to 1mm.
The initial separation between clamping jaws (l_0) was 20mm and at least three samples of [Cu(NH_2-MeIN)I]$_n$@EVA composite with each concentration were tested. Force (F) and displacement (Δl) data for each test were obtained, and then converted to stress-strain using the equations [1 and 2].

$$\sigma = \frac{F}{A_0} \quad \text{(Eq. 1)}; \qquad e = \frac{\Delta l}{l_0} \quad \text{(Eq. 1)}$$

The Young Modulus (E) gives the relationship between Stress (σ) and Strain (e), which has been estimated using equation 3:

$$\sigma = E \cdot e \quad \text{(Eq. 2)}$$

Conflicts of interest

There are no conflicts to declare.

Acknowledgements

This article has been funded by the Spanish Ministerio de Economía y Competitividad (and the current Ministerio de Ciencia, Innovación y Universidades) (MAT2016-75883-C2-2-P, MAT2016-75716-C2-2-Rand RTI2018-095563-B-100). This article is dedicated to J. J. Amo-Mora.

Notes and references

[1] C. Strümpel, M. McCann, G. Beaucarne, V. Arkhipov, A. Slaoui, V. Švrček, C. del Cañizo, I. Tobias, *Sol. Ener. Mater. Sol. Cells* 2007, **91**, 238.

[2] a) S. G. Dunning, A. J. Nuñez, M. D. Moore, A. Steiner, V. M. Lynch, J. L. Sessler, B. J. Holliday, S. M. Humphrey, *Chem.* 2017, ***2***, 579; b) I. A. Ibarra, T. W. Hesterberg, J.S. Chang, J. W. Yoon, B. J. Holliday, S. M. Humphrey, *Chem. Commun.* 2013, **49**, 7156.

[3] M. J. Keevers, M. A. Green, *J. Appl. Phys.* 1994, **75**, 4022.

[4] Z. Chen, G. Wu, H. Jia, K. Sharafudeen, W. Dai, X. Zhang, S. Zeng, J. Liu, R. Wei, S. Lv, G. Dong, J. Qiu, *J. Phys. Chem. C.* 2015, **119**, 24056.

[5] T. Monzón-Hierro, J. Sanchiz, S. González-Pérez, B. Gonzalez-Diaz, S. Holinski, D. Borchert, C. Hernández-Rodríguez, R. Guerrero-Lemus, *Sol. Ener. Mater. Sol. Cells* 2015, 187.

[6] R. Guerrero-Lemus, J. Sanchiz, M. Sierra-Ramos, I. Martin, C. Hernández Rodríguez, D. Borchert, *Sens. Actuators A: Phys.* 2018, **271**, 60.

[7] X. Huang, S. Han, W. Huang, X. Liu, *Chem. Soc. Rev.* 2013, **42**, 173.

[8] a) J. Troyano, J. Perles, P. Amo-Ochoa, F. Zamora, S. Delgado, *Crystengcomm.* 2016, **18**, 1809; b) J. Troyano, J. Perles, P. Amo-Ochoa, J. I. Martínez, M. Concepción Gimeno, V. Fernández-Moreira, F. Zamora, S. Delgado, *Chem. Eur. J.* 2016, **22**, 18017; c) K. Hassanein, J. Conesa-Egea, S. Delgado, O. Castillo, S. Benmansour, J. I. Martinez, G. Abellan, C. J. Gomez-Garcia, F. Zamora, P. Amo-Ochoa, *Chem. Eur. J.* 2015, **21**, 17282; d) K. Hassanein, P. Amo-Ochoa, C. J. Gomez-Garcia, S. Delgado, O. Castillo, P. Ocon, J. I. Martinez, J. Perles, F. Zamora, *Inorg. Chem.* 2015, **54**, 10738.

[9] J. Conesa-Egea, N. Nogal, J. I. Martínez, V. Fernández-Moreira, U. R. Rodríguez-Mendoza, J. González-Platas, C. J. Gómez-García, S. Delgado, F. Zamora, P. Amo-Ochoa, *Chem. Sci.* 2018, **9**, 8000.

[10] G. K. Kole, J. J. Vittal, *Chem. Soc. Rev.* 2013, **42**, 1755.

[11] Z. Hu, B. J. Deibert, J. Li, *Chem. Soc. Rev.* 2014, **43**, 5815.

[12] P. Amo-Ochoa, F. Zamora, *Coord. Chem. Rev.* 2014, **276**, 34.

[13] U. Mueller, M. Schubert, F. Teich, H. Puetter, K. Schierle-Arndt, J. Pastré, *J. Mater. Chem.* 2006, **16**, 626.

[14] B. V. a. M. N. Berberan-Santos, *Wiley-VCH Verlag GmbH & Co* 2012, *2nd edn*.

[15] E. Klampaftis, B. S. Richards, *Prog. Photovoltaics: Research App.* 2011, **19**, 345.

[16] S. Peeterbroeck, M. Alexandre, R. Jérôme, P. Dubois, *Poly. Degrad. Stab.* 2005, **90**, 288.

[17] R. Guerrero-Lemus, J. Sanchiz, M. Sierra-Ramos, I. R. Martín, C. Hernández-Rodríguez, D. Borchert, *Sens. Actuators A: Phys.* 2018, **271**, 60.

[18] L. Yang, D. R. Powell, R. P. Houser, *Dalton T.* 2007, 955.

[19] S. González-Pérez, J. Sanchiz, B. González-Díaz, S. Holinski, D. Borchert, C. Hernández-Rodríguez, R. Guerrero-Lemus, *Surf. Coat. Technol.* 2015, **271**, 106.

[20] T. Fix, A. Nonat, D. Imbert, S. Di Pietro, M. Mazzanti, A. Slaoui, L. J. Charbonnière, *Progr. Photovoltaics: Res. App.* 2016, **24**, 1251.

[21] G. Zucchi, V. Murugesan, D. Tondelier, D. Aldakov, T. Jeon, F. Yang, P. Thuéry, M. Ephritikhine, B. Geffroy, *Inorg. Chem.* 2011, **50**, 4851.

[22] A. W. Czanderna, G. J. Jorgensen, *AIP Conference Proceedings* 1997, **394**, 295.

[23] M. Aklalouch, A. Calleja, X. Granados, S. Ricart, V. Boffa, F. Ricci, T. Puig, X. Obradors, *Sol. Ener. Mater. Sol. Cells* 2014, **120**, 175.

[24] B. González-Díaz, M. Sierra-Ramos, J. Sanchiz, R. Guerrero-Lemus, *Sens. Actuators A: Phys.* 2018, **276**, 312.

[25] E. Klampaftis, M. Congiu, N. Robertson, B. S. Richards, *IEEE J. Photovoltaics* 2011, **1**, 29.

[26] T. Monzón-Hierro, J. Sanchiz, S. González-Pérez, B. González-Díaz, S. Holinski, D. Borchert, C. Hernández-Rodríguez, R. Guerrero-Lemus, *Sol. Ener. Mater.Solar Cells* 2015, **136**, 187.